

十二烷基硫酸钠水溶液液滴在微凹槽阵列 PDMS 表面上的电润湿行为实验研究

廖洋波^{1a}, 黄先富^{2,3}, 卢应发^{1a}, 余迎松^{1a,1b,1c*}

(1.湖北工业大学 a.土木建筑与环境学院 b.河湖健康智慧感知与生态修复教育部重点实验室 c.生态环境岩土与河湖生态修复学科引智创新示范基地, 武汉 430068; 2.中国科学院力学研究所 非线性力学国家重点实验室, 北京 100190; 3.广东空天科技研究院(南沙), 广州 511458)

摘要: **目的** 研究十二烷基硫酸钠 (Sodium dodecyl sulfate, SDS) 水溶液液滴在微凹槽阵列聚二甲基硅氧烷 (Polydimethylsiloxane, PDMS) 表面的电润湿行为特征。**方法** 采用注入析出法, 测量含 KCl 的 SDS 水溶液液滴在微凹槽阵列非浸润表面的接触角滞后。通过施加直流电压, 研究 SDS 浓度和表面粗糙度对含 KCl 的 SDS 水溶液液滴的电润湿行为的影响。**结果** 微凹槽阵列非浸润表面表现出较强的润湿各向异性, 与平行于微凹槽方向上的表观接触角 ($110^{\circ} \leq \theta_e \leq 141^{\circ}$)、前进角 ($116^{\circ} \leq \theta_a \leq 144^{\circ}$) 和后退角 ($99^{\circ} \leq \theta_r \leq 137^{\circ}$) 相比, 垂直于微凹槽方向上的表观接触角 ($142^{\circ} \leq \theta_e \leq 165^{\circ}$)、前进角 ($159^{\circ} \leq \theta_a \leq 177^{\circ}$) 和后退角 ($118^{\circ} \leq \theta_r \leq 140^{\circ}$) 普遍更大。当表面固定时, 水溶液液滴电润湿的启动电压和饱和电压, 以及发生润湿状态转变所需的电压均随着 SDS 浓度的增加而减小。当水溶液中 SDS 的浓度固定时, 沿垂直于凹槽方向的启动电压随着固相分数的减小而减小, 沿平行于凹槽方向的启动电压随着固相分数的减小而增大, 而饱和电压均随着固相分数的减小而减小。**结论** 添加十二烷基硫酸钠可以有效降低 SDS 水溶液液滴电润湿的启动电压和电润湿过程中水溶液液滴在微凹槽 PDMS 表面润湿状态转变所需的电压, 使得 SDS 水溶液液滴在微凹槽阵列 PDMS 表面的电润湿行为发生了改变。

关键词: 十二烷基硫酸钠; 液滴; 启动电压; 饱和电压; 表面粗糙度; 接触角滞后

中图分类号: O369; TB34 **文献标识码:** A **文章编号:** 1001-3660(2023)12-0178-10

DOI: 10.16490/j.cnki.issn.1001-3660.2023.12.016

Experimental Investigation of Electrowetting of Aqueous Sodium Dodecyl Sulfate Droplets on Micro-grooved Non-wetting Surfaces

LIAO Yang-bo^{1a}, HUANG Xian-fu^{2,3}, LU Ying-fa^{1a}, YU Ying-song^{1a,1b,1c*}

(1. a. School of Civil Engineering, Architecture and Environment, b. Key Laboratory of Intelligent Health Perception and Ecological Restoration of Rivers and Lakes, c. Innovation Demonstration Base of Ecological Environment, Geotechnical and Ecological Restoration of Rivers and Lakes, Hubei University of Technology, Wuhan 430068, China;

收稿日期: 2023-08-20; 修订日期: 2023-10-09

Received: 2023-08-20; Revised: 2023-10-09

基金项目: 国家自然科学基金(11572114); 生态环境岩土与河湖生态修复学科引智创新示范基地(2020EJB004); 广东省基础与应用基础研究基金(2023A1515011784); 广东省高水平创新研究院项目(2020B0909010003)

Fund: National Natural Science Foundation of China (11572114); Innovation Demonstration Base of Ecological Environment Geotechnical and Ecological Restoration of Rivers and Lakes (2020EJB004); Guangdong Basic and Applied Basic Research Foundation (2023A1515011784); High-level Innovation Research Institute Program of Guangdong Province (2020B0909010003)

引文格式: 廖洋波, 黄先富, 卢应发, 等. 十二烷基硫酸钠水溶液液滴在微凹槽阵列 PDMS 表面上的电润湿行为实验研究[J]. 表面技术, 2023, 52(12): 178-187.

LIAO Yang-bo, HUANG Xian-fu, LU Ying-fa, et al. Experimental Investigation of Electrowetting of Aqueous Sodium Dodecyl Sulfate Droplets on Micro-grooved Non-wetting Surfaces[J]. Surface Technology, 2023, 52(12): 178-187.

*通信作者 (Corresponding author)

2. State Key Laboratory of Nonlinear Mechanics, Institute of Mechanics, Chinese Academy of Sciences, Beijing 100190, China; 3. Guangdong Aerospace Research Academy (Nansha), Guangzhou 511458, China)

ABSTRACT: Electrowetting on dielectric (EWOD) has found wide applications in micro-/nano-fluidics for its precise and accurate manipulation of minor droplets. Micro-grooved non-wetting surfaces exhibit great anisotropy in surface wettability and have been used as surfaces for directional transport of liquid. The work aims to study the electrowetting characteristics of aqueous sodium dodecyl sulfate (SDS) aqueous droplets on micro-grooved polydimethylsiloxane (PDMS) surfaces, which were obtained by the peeling-off method. The solid fraction of micro-grooved PDMS surfaces was 0.50, 0.33 and 0.20, respectively. SDS concentration was fixed at 0, 0.41, 0.82, 1.23 and 1.62 mmol/L, respectively. Firstly, wettability of SDS aqueous droplets containing 1 mmol/L KCl on micro-grooved PDMS surfaces without the application of a direct current (DC) electric field was measured. It was found that all droplets were at the Cassie-Baxter wetting state, micro-grooved surfaces exhibited a strong anisotropy in surface wettability, and the apparent, advancing and receding contact angles were all larger in the transverse direction than the corresponding values in the longitudinal direction. Secondly, electrowetting of aqueous SDS droplets containing 1 mmol/L KCl on micro-grooved PDMS surfaces was experimentally studied by varying SDS concentration and surface roughness of the substrate. Platinum wire was inserted into the mixture droplet as an electrode and micro-grooved PDMS surfaces were placed on the conducting layer of ITO glass. DC electric field was applied to the system at the increase speed of 20 V/s and droplet shape analyzer DSA30 was adjusted as soon as possible to record the profile of sessile droplets at the speed of 1 frame per second. The non-wetting surface of micro-grooved array showed strong wettability anisotropy. Compared with the apparent contact angle ($110^\circ \leq \theta_e \leq 141^\circ$), advancing angle ($116^\circ \leq \theta_a \leq 144^\circ$) and retreating angle ($99^\circ \leq \theta_r \leq 137^\circ$) in the longitudinal direction, the apparent contact angle ($142^\circ \leq \theta_e \leq 165^\circ$), advancing angle ($159^\circ \leq \theta_a \leq 177^\circ$) and retreating angle ($118^\circ \leq \theta_r \leq 140^\circ$) in the transverse direction were larger. It was found that there existed two characteristic values of applied voltage. The first one was the actuation voltage, which was widely accepted to be related to contact angle hysteresis. Another one was the saturation voltage which might originate from the trapping of charge. In this work, it was found that actuation voltage for SDS aqueous droplets was more sensitive along the longitudinal direction, indicating that there was less contact angle hysteresis along the longitudinal direction than along the transverse direction because more energy was needed to be overcome when the droplets spread along the transverse direction. Actuation voltage was found to decrease with increasing SDS concentration. Moreover, saturation voltage and the voltage for the transition from the Cassie-Baxter wetting state to the Wenzel one were also found to both decrease with the increase of SDS concentration. At the same time, actuation voltage of droplets along the longitudinal direction was found to decrease with the decrease of the solid fraction of micro-grooved PDMS surfaces, while actuation voltage of droplets along the transverse direction increased with the decrease of the solid fraction of micro-grooved PDMS surfaces. Moreover, saturation voltage decreased with the decrease of the solid fraction. Besides, for the case of micro-grooved surfaces with a solid fraction of 0.20 or 0.33, it was observed that a phenomenon of multistage stepped reduction in the instantaneous contact angle along the transverse direction was observed and it could be attributed to the fact that more energy barrier due to contact angle hysteresis must be overcome when the droplets spread in the direction perpendicular to the microgrooves. It can be concluded that addition of SDS molecules into liquid can effectively reduce the actuation voltage and the applied voltage necessary for the wetting transition, resulting in the variation of characteristics of electrowetting of aqueous SDS droplets on micro-grooved PDMS surfaces.

KEY WORDS: sodium dodecyl sulfate; droplet; actuation voltage; saturation voltage; surface roughness; contact angle hysteresis

电润湿 (Electrowetting, EW) 指在液滴中施加直流/交流电压, 使液滴在固体表面的润湿性能发生变化的一种现象, 在微流体芯片^[1]、石油开采^[2]、化工洁净^[3]等方面得到了广泛应用, 近 20 年来受到了世界各国学者的高度重视。电润湿现象可以追溯到 1875 年 Lippmann 发现的电毛细现象^[4]。为了尽量消除电解的发生, 1993 年 Berge 在电润湿模型中引入介

电层, 被称为介质上的电润湿 (Electrowetting-on-dielectric, EWOD)^[5]。电润湿通过施加电压控制液滴的接触角, 当增大外加电压时, 接触角 (Contact angle, CA) 减小; 相反, 当施加的电压降低时, 接触角增大。表观接触角与外加电压之间的关系可以用

Lippmann-Young 方程描述, $\cos \theta = \cos \theta_0 + \frac{\epsilon \epsilon_0 V^2}{2 \gamma_{lv} d}$ 。

式中, θ_0 、 V 、 ε 、 ε_0 、 γ_{lv} 、 d 分别表示本征接触角、外加电压、介电层相对介电常数、真空介电常数、液-气界面张力和介电层厚度^[6-7]。

目前,液滴在一般粗糙表面^[8]、曲面^[9]和有序粗糙表面^[10]的电润湿都得到了重视,同时液滴在各向异性表面上的电润湿研究也正在发展^[11]。微凹槽阵列表面拥有极强的各向异性,因此广泛应用于液滴的定向运输^[12]、防水^[13]、集水^[14]和冷凝传热增强^[15]等领域。当液滴沉积在微凹槽阵列表面时,液滴将沿凹槽被拉长,形成椭圆或椭圆状的三相接触线^[16-17],并且在2个方向上具有不同的表观接触角,通常垂直于微凹槽的表观接触角比平行于微凹槽的表观接触角大^[12]。

液滴附着于微结构表面时,存在3种表面润湿状态,当液体完全占据微结构之间的空腔时,液滴处于Wenzel润湿状态^[18];当液滴位于微结构表面时,液滴处于Cassie-Baxter润湿状态^[19];当液滴在微结构表面部分处于Wenzel润湿状态,其余部分为Cassie-Baxter润湿状态时,液滴为混合润湿状态^[20]。事实上,纯粹的Wenzel润湿状态和Cassie-baxter润湿状态是罕见的^[21]。当施加外部压力^[22],如振动^[23]、表面声波^[24]时,液滴可由Cassie-baxter润湿状态过渡到Wenzel润湿状态。

表面活性剂含有1个亲水基团及1个或多个疏水基团,可有效降低液体的表面张力,在调控润湿摩擦因数^[25]、调控沸腾气泡成核^[26]、改善电极表面油脂去除效果^[27]等方面也得到广泛应用。表面活性剂对液滴电润湿起到了很大作用,近20多年来世界各国学者开展了表面活性剂水溶液液滴在介电层上电润湿行为的研究^[27-31]。研究表明,表面活性剂的添加可以显著降低液滴电润湿所需的电压,提升安全性和经济性。目前,还无关于十二烷基硫酸钠水溶性液滴在由微凹槽阵列构成的疏水表面电润湿的研究。文中使用倒模法制备微凹槽阵列PDMS膜,并配置含有KCl的SDS水溶液,先后进行水溶液液滴在微凹槽非润湿性表面的滞后与电润湿实验,研究表面活性剂浓度和微凹槽阵列的固相分数对液滴电润湿的影响,并在实验中观察液滴的润湿状态转变过程,拟为电润湿应用领域的拓展提供理论参考。

1 实验

1.1 材料与仪器

1.1.1 基底制备

采用倒模法^[32],制作微凹槽阵列PDMS(Dow Europe GmbH C/O Dow Silicones Deutschland GmbH, Dowsil™ 184,德国)膜。具体步骤:将微结构硅片依次放入无水乙醇、丙酮和去离子水中超声清洗

10 min,以清洁微结构硅片;待微结构硅片静置风干后,对其进行等离子处理和硅烷化处理,然后在其表面旋涂PDMS基底与固化剂的质量比为10:1的PDMS胶质;再将旋涂后的硅片放入真空干燥箱里抽真空30 min,以去除胶质与微结构硅片之间的气泡;之后将其放入烘箱,在90℃下烘4 h;待样品冷却后,使用镊子和手术刀小心地进行剥离,即可得到微凹槽阵列PDMS膜。

制备基底时使用的仪器主要包括等离子清洗机(Mycro, PDC-002,美国)、匀胶旋涂仪(Laurell, WS-650MZ-23NPPB,美国)、真空干燥箱、鼓风烘箱、电子天平(精度为1 mg)等。

1.1.2 化学剂及溶液配制

将SDS(Aladdin,中国)、KCl(沪试SCR,中国)和去离子水按照一定比例混合成溶液,使混合后的溶液中KCl的浓度固定为1 mmol/L,而SDS的浓度分别为0、0.41、0.82、1.23、1.64 mmol/L。已有文献报道,盐分的加入会改变表面活性剂的临界胶束浓度^[33]。经计算,当KCl的浓度为1 mmol/L时,含KCl的SDS水溶液的临界胶束浓度在25℃时为7.3 mmol/L(不含盐分的SDS水溶液的临界胶束浓度在25℃时约为8.2 mmol/L^[34])。配置好的溶液需在24 h内使用完毕。如无特别说明,文中的“SDS水溶液”均含有1 mmol/L的KCl。

1.2 表征

采用激光扫描共聚焦显微镜(Zeiss, LSM900,德国)对微凹槽阵列PDMS基底的表面微观形貌和三维轮廓进行观测,使用液滴形貌分析仪(Krüss, DSA30,德国)进行接触角的测量。

1.3 方法

表面润湿性能实验:使用液滴形貌分析仪(Krüss, DSA30,德国)测量SDS水溶液液滴在平坦PDMS表面和微凹槽阵列PDMS表面的接触角。采用注入析出法^[35]测量SDS水溶液液滴在微凹槽阵列PDMS表面的前进接触角和后退接触角。实验时环境温度为 $(24 \pm 2)^\circ\text{C}$,相对湿度为 $(15 \pm 2)\%$ 。分别从垂直于微凹槽方向和平行于微凹槽方向对其表面润湿性能进行测量,并且每个实验至少重复3次,以确保其准确性。为简便起见,文中将垂直于微凹槽方向和平行于微凹槽方向分别简写为T、L。

电润湿实验:将微凹槽阵列PDMS膜黏附在ITO导电玻璃的导电层上,并尽可能保证粘贴的紧密性。调整ITO导电玻璃,使得微凹槽阵列平行或垂直于接触角测量仪的拍摄方向,随后固定ITO导电玻璃,并连接电源,准备通电。

使用NE30针头将名义体积为2.0 μL 的SDS水

溶液液滴缓慢沉积在微凹槽阵列 PDMS 膜上, 将直径为 0.1 mm 的铂丝插入液滴中央, 同时避免接触微结构表面。通过高压功率放大器 (Trek, 677B, 美国) 以 20 V/s 的增幅对系统施加直流电压, 并以 1 帧/s 的速度记录液滴的轮廓, 直至液滴接触角达到饱和。实验时环境温度为 $(17 \pm 2)^\circ\text{C}$, 相对湿度为 $(20 \pm 2)\%$ 。基于微凹槽表面的各向异性, 分别从 L 和 T 2 个方向对液滴进行观察, 2 个方向的表现接触角分别用 θ_L 和 θ_T 表示。每个实验至少重复 3 次, 以确保其准确性。实验装置示意图如图 1 所示。

2 结果与讨论

2.1 微凹槽阵列 PDMS 表面形貌观测

通过激光扫描共聚焦显微镜观察微凹槽阵列表面的微观形貌。经测量, 所有微凹槽阵列的间距 S 和深度 H 均为 20 μm , 微凹槽宽度 W 分别为 20、40、80 μm , 如图 2 所示。使用固相分数 ϕ ($\phi = \frac{S}{W+S}$) 和表面粗糙度 R_f ($R_f = 1 + \frac{2H}{W+S}$) 来表征这些表面, 相应数值列于表 1。

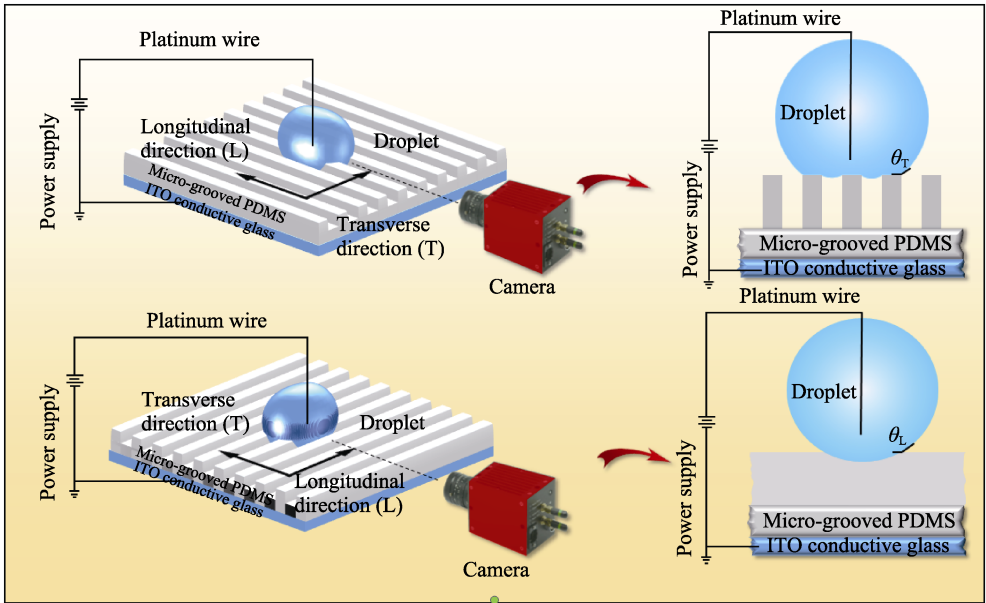


图 1 电润湿实验装置示意图
Fig.1 Schematic diagram of the experimental apparatus for electrowetting

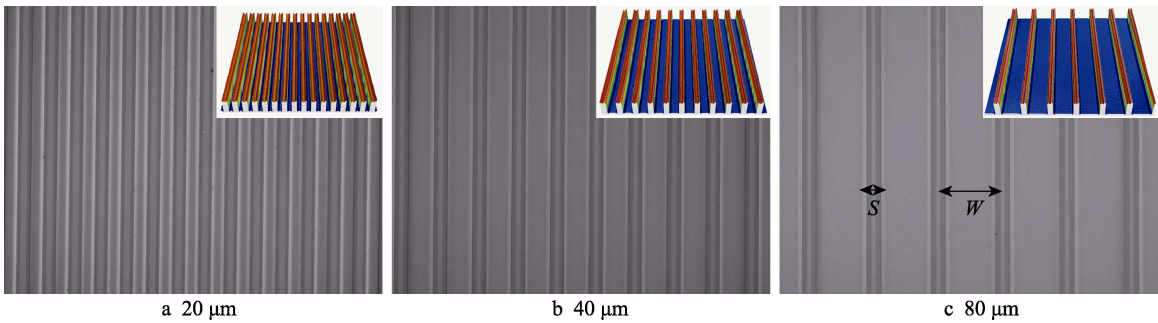


图 2 微凹槽阵列 PDMS 表面的激光共聚焦显微镜表征
Fig.2 LSCM characterization of the micro-grooved PDMS surface

表 1 实验中所用的样品参数
Tab.1 Parameters of samples used in the experiments

$S/\mu\text{m}$	$H/\mu\text{m}$	$W/\mu\text{m}$	ϕ	R_f
20	20	20	0.50	2
20	20	40	0.33	1.67
20	20	80	0.20	1.4

2.2 SDS 水溶液液滴在微凹槽阵列 PDMS 表面上的润湿性能

SDS 水溶液液滴在微凹槽阵列 PDMS 表面上的表现接触角 θ_e 、前进接触角 θ_a 和后退接触角 θ_r 如表 2 所示。其中, θ_{CB} 为水溶液液滴在 Cassie-Baxter 润湿状态下的理论初始接触角, $\cos \theta_{CB} = \phi \cos \theta_0 - (1 - \phi)^{[18-19]}$,

表 2 SDS 水溶液液滴在微凹槽阵列 PDMS 表面的润湿性能
Tab.2 Wettability of SDS aqueous droplets on micro-grooved PDMS surfaces

ϕ	$C_{\text{SDS}}/(\text{mmol}\cdot\text{L}^{-1})$	$\theta_0/(\circ)$	$\theta_{\text{CB}}/(\circ)$	$\theta_c/(\circ)$		$\theta_a/(\circ)$		$\theta_r/(\circ)$	
				L	T	L	T	L	T
0.50	0	109±2	131±2	123±2	142±2	132±2	159±2	109±2	118±2
	0.41	105±2	129±2	120±	144±2	128±2	159±2	106±2	120±2
	0.82	95±2	122±2	117±2	146±2	124±2	159±2	104±2	122±2
	1.23	91±2	120±2	112±2	149±2	119±2	160±2	100±2	126±2
	1.62	88±2	118±2	110±2	151±2	116±2	161±2	99±2	128±2
0.33	0	109±2	141±2	131±2	146±2	138±2	164±2	118±2	121±2
	0.41	105±2	139±2	128±2	150±2	135±2	166±2	115±2	125±2
	0.82	95±2	134±2	126±2	153±2	132±2	166±2	114±2	129±2
	1.23	91±2	132±2	124±2	155±2	130±2	167±2	112±2	131±2
	1.62	88±2	131±2	123±2	159±2	126±2	170±2	111±2	136±2
0.20	0	109±2	149±2	141±2	156±2	144±2	175±2	137±2	130±2
	0.41	105±2	148±2	140±2	159±2	141±2	176±2	136±2	133±2
	0.82	95±2	144±2	139±2	161±2	140±2	176±2	135±2	135±2
	1.23	91±2	143±2	138±2	164±2	139±2	177±2	135±2	138±2
	1.62	88±2	142±2	136±2	165±2	137±2	177±2	133±2	140±2

式中 θ_0 为液滴在平坦的 PDMS 表面的本征接触角。由表 2 可见,水溶液液滴在微凹槽阵列 PDMS 表面上的润湿性能表现出强烈的各向异性,沿 T 方向的表现接触角、前进角相较于沿 L 方向的均更大,且由 Cassie-Baxter 模型计算得到的接触角 θ_{CB} 介于沿 T、L 方向的接触角之间,表明水溶液液滴此时处于 Cassie-Baxter 润湿状态。当表面的固相分数一定时,随着 SDS 浓度的增加,沿 L 方向的表现接触角、前进角和后退角均逐渐减小,但是沿 T 方向的表现接触角、前进角和后退角均逐渐增大。这主要是因当液滴沿 T 方向润湿时需要克服更大的能垒。当 SDS 水溶液液滴中 SDS 的浓度一定时,随着固相分数的降低,无论是沿 L 方向还是 T 方向的表现接触角、前进角和后退角均逐渐增大。

2.3 不同浓度的 SDS 水溶液液滴在微凹槽阵列 PDMS 表面上的电润湿

不同浓度的 SDS 水溶液液滴在微凹槽阵列 PDMS

表面沿 L、T 这 2 个方向的瞬时接触角随电压的变化曲线如图 3~4 所示。由图 3~4 可见,当电压增大到一定值时,瞬时接触角才开始逐渐随着电压的增大而减小,该电压定值被称为启动电压。沿着 L 方向,启动电压随着 SDS 浓度的增加逐渐减小,其中以固相分数为 0.50 时启动电压的减小趋势最明显。沿着 T 方向,启动电压也随着 SDS 浓度的增加逐渐减小,但是减小趋势相较于 L 方向明显偏小,表明 SDS 的浓度对沿 T 方向的接触角滞后的影响并不突出。已有研究表明,启动电压与液滴在固体表面的接触角滞后相关^[36]。可以推测,在电场作用下,SDS 水溶液液滴在微凹槽阵列 PDMS 表面沿 L 方向的接触角滞后随着 SDS 浓度的增大而减小,但是 SDS 浓度对沿 T 方向的接触角滞后无明显影响。值得注意的是,沿 T 方向的初始接触角随着 SDS 浓度的增大而增大,这一行为十分反常,其作用机理还有待进一步研究。当继续施加电压直至饱和电压^[37]后,瞬时接触角将不再随电压的增加而减小,且饱和电压随 SDS 浓度的增大而

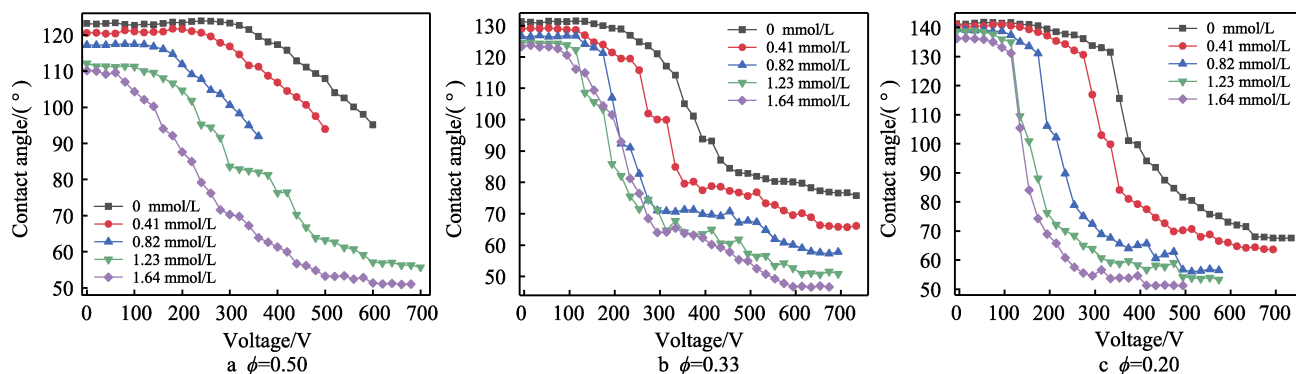


图 3 不同浓度的 SDS 水溶液液滴在微凹槽阵列 PDMS 表面沿 L 方向的电润湿曲线
Fig.3 Electrowetting curves of SDS aqueous droplets of different concentrations in the L direction of micro-grooved PDMS surfaces

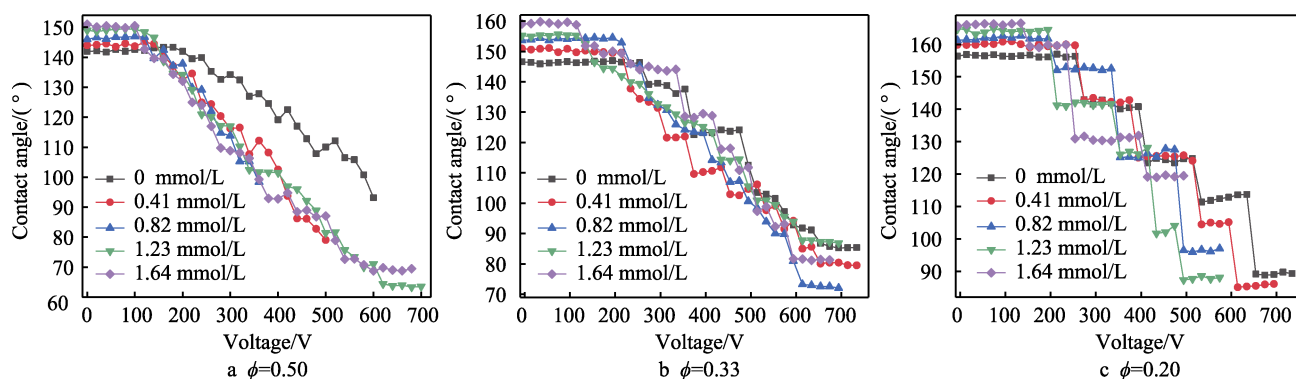


图 4 不同浓度的 SDS 水溶液液滴在微凹槽阵列 PDMS 表面上沿 T 方向的电润湿曲线

Fig.4 Electrowetting curves of SDS aqueous droplets of different concentrations in the T direction of micro-grooved PDMS surfaces

减小。目前, 饱和电压的形成未形成定论, 发生这种现象可能因三相接触线附近逐渐增加的电场超过了介电层的电绝缘能力, 随后电荷被捕获在介电层上, 而介电层中被捕获的电荷不会产生电润湿效应, 从而导致接触角不再变化^[37]。

当施加电压超过启动电压时, 沿 L 方向的瞬时接触角逐渐随电压的增大而减小, 但沿 T 方向的瞬时接触角随电压的增加出现多级台阶状减小现象, 如图 4 所示。其中, 以固相分数为 0.33、0.20 时多级台阶状减小现象最明显。这是由于液滴向 T 方向铺展时, 系统内部不断积累的势能克服了由接触角滞后引起的能垒, 当液滴克服第 1 个能垒时, 系统内部残余的势能将促使液滴迅速向 T 方向铺展, 直至遇到第 2 个能垒。此时, 系统内部需继续积累势能, 以克服第 2 个能垒, 循环往复, 导致多级台阶接触角的形成, 这种现象直至液滴接触角不再变化时结束。

对于固相分数为 0.50 的表面, 当 SDS 浓度为 0、0.41、0.82 mmol/L, 电压增至某固定值时, 液滴出现了弹飞现象(如图 5 所示)。由图 5 可见, 将 1 mmol/L KCl 水溶液液滴 (SDS 浓度为 0 mmol/L) 在固相分数为 0.50 表面上进行电润湿实验, 当施加 600 V 电

压时液滴和导电铂丝还处于连接状态, 此时液滴未受到电场的影响; 当施加 620 V 电压时, L 方向的液滴脱离铂丝的连接, 向左发生偏移, T 方向液滴的图像已经模糊, 并可见明显的前后偏移现象, 说明此时沿着微凹槽方向发生了液滴弹飞现象。发生这种现象的原因可能是在电润湿时, 液滴的面电荷密度不均匀, 导致外加电场在液滴三相接触线处诱导的 Maxwell 应力不尽相同, 液滴沿着三相接触线上所有 Maxwell 应力的合力超过了三相接触线处的钉扎力, 与此同时表面微结构给予液滴较大的能垒, 使得液滴较难跨越微凹槽纹理, 从而迫使液滴沿着微凹槽方向出现弹飞现象。

在不同固相分数的微凹槽阵列 PDMS 表面, SDS 水溶液液滴沿着 L、T 这 2 个方向的瞬时接触角随着电压的变化曲线如图 6~7 所示。由图 6~7 可见, 沿着 L 方向, 启动电压随着微凹槽阵列 PDMS 固相分数的减小而逐渐减小, 其减小速度随着 SDS 浓度的增加而减小, 直到 SDS 浓度为 1.64 mmol/L 时 3 种固相分数表面上液滴的启动电压相等, 这表明 SDS 浓度对沿 L 方向的接触角滞后有着较显著的影响。沿着 T 方向, 随着微凹槽阵列 PDMS 固相分数的减小,

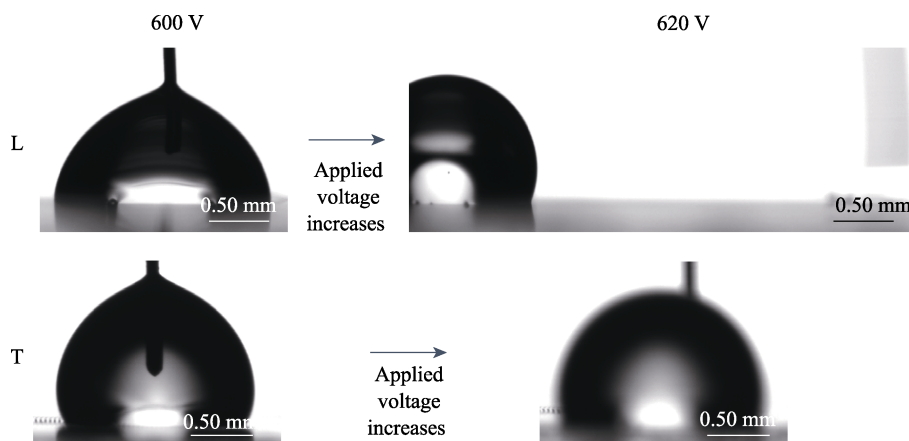


图 5 1 mmol/L KCl 水溶液液滴在固相分数为 0.50 表面上电润湿时液滴的弹飞现象

Fig.5 Ricochet phenomenon of 1 mmol/L KCl aqueous droplets during electrowetting on a surface with a solid fraction of 0.50

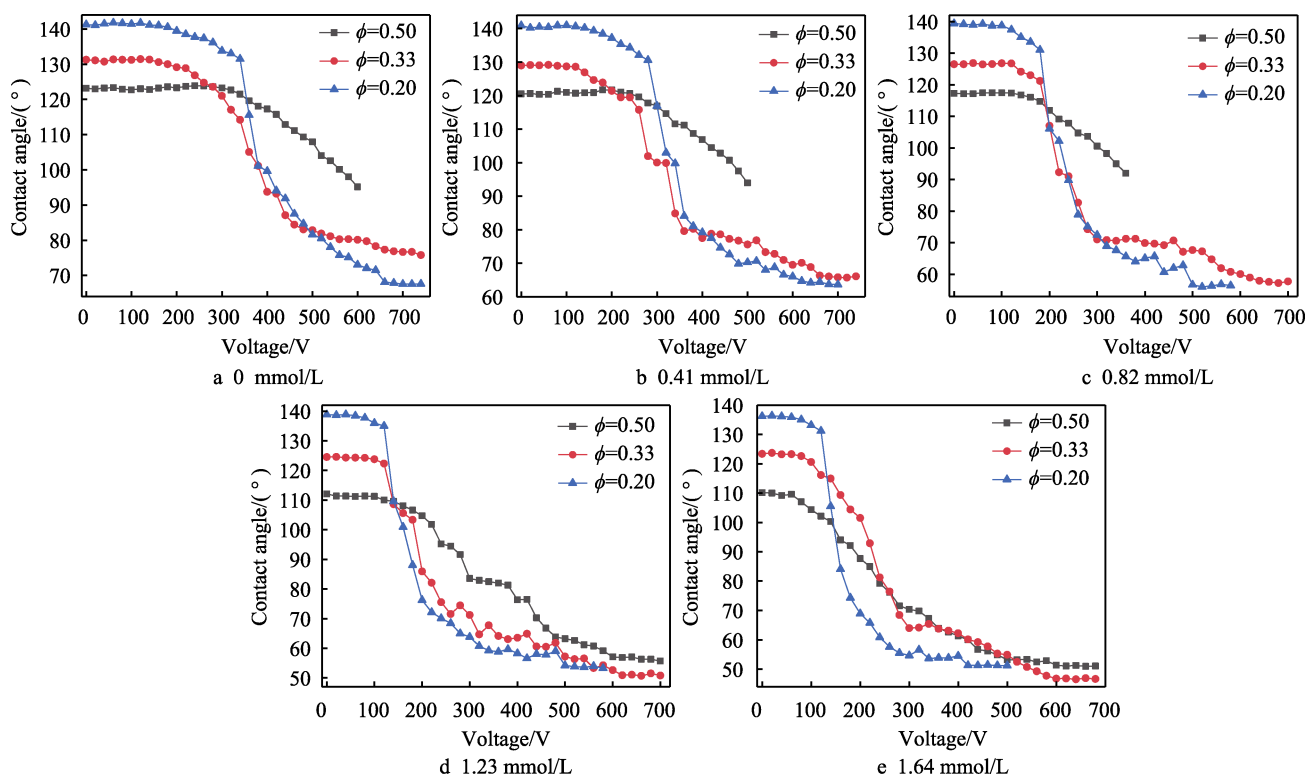


图6 SDS水溶液液滴在不同固相分数的微凹槽阵列PDMS表面上沿L方向的电润湿曲线

Fig.6 Electrowetting curves of SDS aqueous droplets in the L direction of micro-grooved PDMS surfaces with different solid fractions

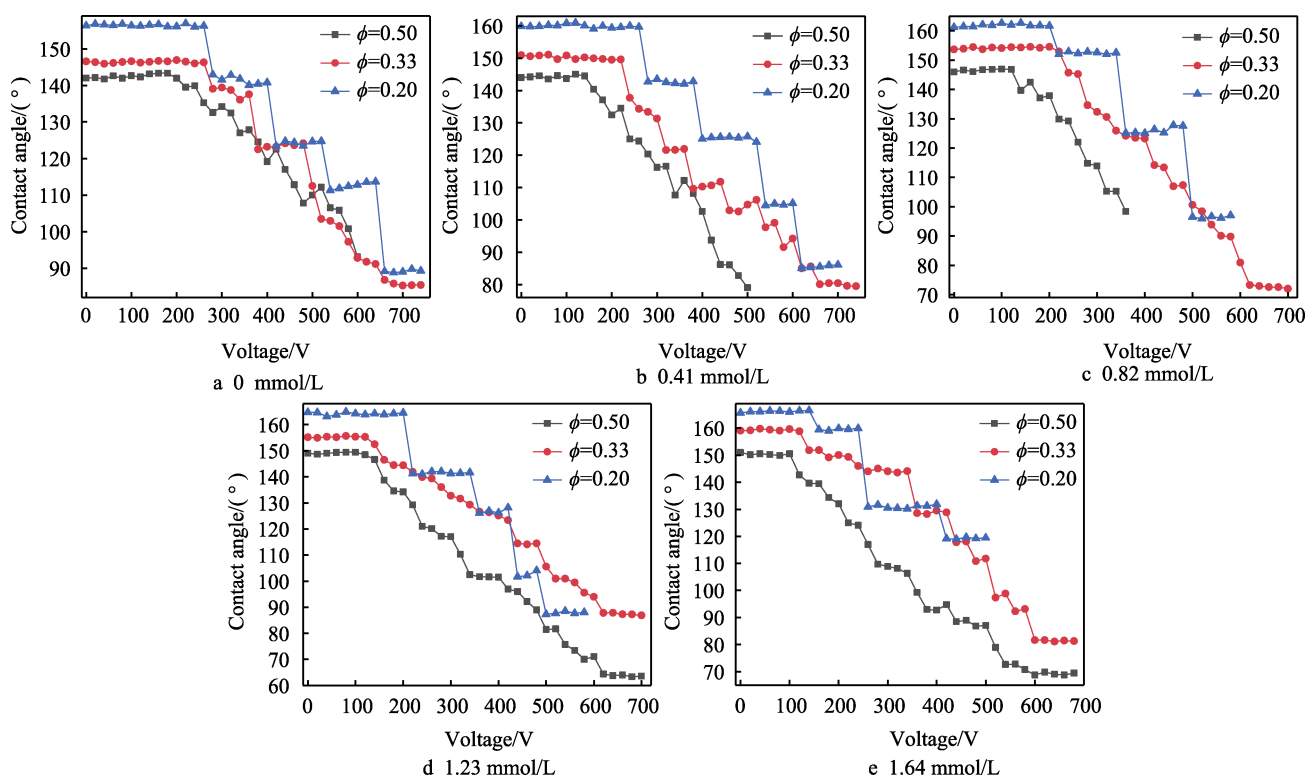


图7 SDS水溶液液滴在不同固相分数的微凹槽阵列PDMS表面上沿T方向的电润湿曲线

Fig.7 Electrowetting curves of SDS aqueous droplets in the T direction of micro-grooved PDMS surfaces with different solid fractions

微凹槽的宽度增大,液滴在电润湿时需要克服的能垒增大,导致启动电压增大,饱和电压也随着微凹槽阵列PDMS固相分数的减小而减小。

2.4 液滴电润湿时润湿状态转变现象

SDS水溶液液滴在固相分数为0.20的微凹槽阵列

列 PDMS 表面的电润湿实验快照如图 8 所示。未施加电压时, 液滴底部与基底之间存在明显间隙, 表明此时 SDS 水溶液液滴在微凹槽阵列表面以 Cassie-Baxter 润湿状态存在。施加电压后, 液滴受到了 Maxwell 应力和 Laplace 压力的共同作用, 且 Maxwell 应力随着电压的增大不断增大。当电压施加到某固定值后, 在竖直方向的 Maxwell 应力和 Laplace 压力的共同作用下液体逐渐向凹槽内部渗入, 使得液滴从 Wenzel 润湿状态转变为 Cassie-Baxter 润湿状态, 而

水平方向的 Maxwell 应力促使液体向外铺展, 以减小接触角^[11]。同时, 液滴由 Cassie-Baxter 润湿状态向 Wenzel 润湿状态转变时需要克服一个能垒, 该能垒会产生一个向上的压力, 以抑制液体的向下渗入。当 Maxwell 应力与 Laplace 压力之和大于由能垒引起的压强时, 液体将自行向下渗入, 并促使其润湿状态发生变化^[36,38]。整体来看, SDS 水溶液液滴发生润湿状态转变所需的电压均随着 SDS 浓度的增大而减小。

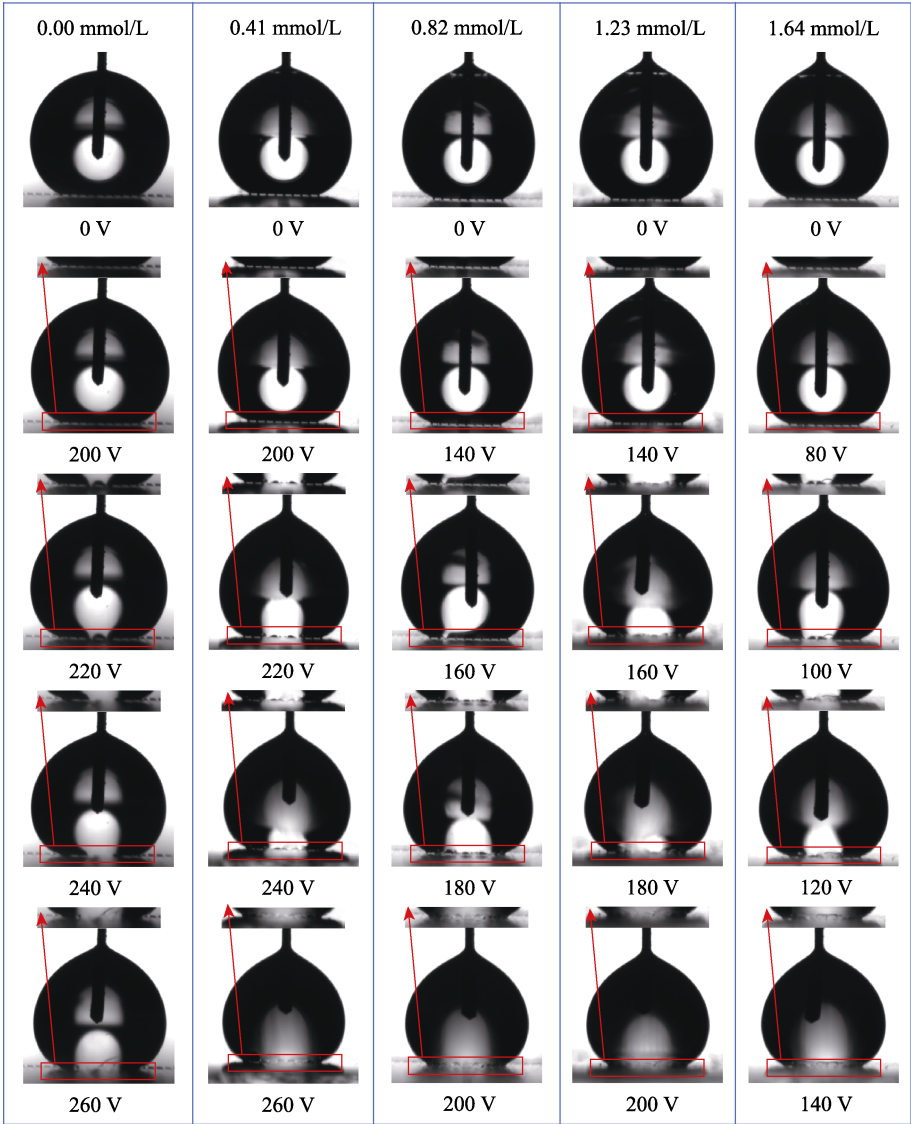


图 8 SDS 水溶液液滴在固相分数为 0.20 的微凹槽阵列 PDMS 表面上沿 T 方向上的电润湿实验快照

Fig.8 Snapshots of electrowetting of SDS aqueous droplets in the T direction of micro-grooved PDMS surface with a solid fraction of 0.20

3 结论

1) SDS 水溶液液滴在微凹槽阵列 PDMS 表面上的润湿性能表现出强烈的各向异性, 沿 T 方向的表现接触角、前进角和后退角相较于沿 L 方向的均更大。

当表面的固相分数一定时, 随着水溶液中 SDS 浓度的增大, 沿 L 方向的表现接触角、前进角和后退角均逐渐减小, 但是沿 T 方向的表现接触角、前进角和后退角均逐渐增大。

2) 液滴电润湿的启动电压和饱和电压随着 SDS

浓度的增大而减小,其中固相分数为 0.50 的表面上启动电压减小的趋势更明显。沿 T 方向液滴的启动电压随着 SDS 浓度的增大而减小的趋势相较于沿 L 方向的明显偏小。固相分数为 0.33、0.20 的微凹槽表面沿 T 方向上液滴接触角随电压的增加而减小时,出现了明显的多级台阶状减小现象。在固相分数为 0.50 的表面,当 SDS 的浓度为 0、0.41、0.82 mmol/L,且电压增大到某极限值时出现了液滴弹飞的现象。

3) 沿 L 方向,液滴的启动电压随着微凹槽表面固相分数的减小而减小,其中 SDS 的浓度为 1.64 mmol/L 时,3 种固相分数的表面启动电压相等。沿 T 方向液滴的电润湿启动电压随着微凹槽表面固相分数的减小而增大,而饱和电压均随着固相分数的减小而减小。

4) 未施加电压时,水溶液液滴在微凹槽阵列 PDMS 表面以 Cassie-Baxter 润湿状态存在。施加电压后,液滴因受到了 Maxwell 应力和 Laplace 压力的共同作用,促使液体逐渐向凹槽内部渗入,直到液滴由 Cassie-Baxter 润湿状态转变为 Wenzel 润湿状态,且 SDS 水溶液液滴发生润湿状态转变所需的电压均随着 SDS 浓度的增大而减小。

参考文献:

- [1] POLLACK M G, SHENDEROV A D, FAIR R B. Electrowetting-Based Actuation of Droplets for Integrated Microfluidics[J]. Lab on a Chip, 2002, 2(2): 96-101.
- [2] CHEN Q G, LIANG W, SONG C H. Effect of Electric Field Strength on Crude Oil Emulsion's Demulsification and Dehydration[J]. High Voltage Engineering, 2014, 40(1): 173-180.
- [3] CHEN P, XU J L, MENG G Y, et al. Influence of Oil Droplet Behavior in Electrochemical Micromembrane Cells on Treating Oil/Water Emulsions with Low-Salt Concentrations[J]. Science of the Total Environment, 2021, 781: 146633.
- [4] BERTHIER J. Microdrops and Digital Microfluidics[M]. New York: William Andrew Inc New York, 2008: 161.
- [5] BERGE B. Electrocapillarite et Mouillage de Films Isolants Par l'eau[J]. Comptes Rendus de l'Academie des Sci Paris Serie, 1993, 317(2): 157-63.
- [6] MUGELE F, BARET J C. Electrowetting: from Basics to Applications[J]. Journal of Physics: Condensed Matter, 2005, 17(28): R705.
- [7] QUILLIET C, BERGE B. Electrowetting: a Recent Outbreak[J]. Current Opinion in Colloid & Interface Science, 2001, 6(1): 34-39.
- [8] MUGELE F. Fundamental Challenges in Electrowetting: from Equilibrium Shapes to Contact Angle Saturation and Drop Dynamics[J]. Soft Matter, 2009, 5(18): 3377-3384.
- [9] WANG Y, ZHAO Y P. Electrowetting on Curved Surfaces[J]. Soft Matter, 2012, 8(9): 2599-2606.
- [10] ZHAO Y P, YUAN Q. Statics and Dynamics of Electrowetting on Pillar-Arrayed Surfaces at the Nanoscale[J]. Nanoscale, 2015, 7(6): 2561-2567.
- [11] WANG Z L, ZHAO Y P. Wetting and Electrowetting on Corrugated Substrates[J]. Physics of Fluids, 2017, 29(6): 067101.
- [12] XIA D, JOHNSON L M, LÓPEZ G P. Anisotropic Wetting Surfaces with One-Dimensional and Directional Dstructures: Fabrication Approaches, Wetting Properties and Potential Applications[J]. Advanced Materials, 2012, 24(10): 1287-1302.
- [13] XIANG Y, HUANG S, HUANG T Y, et al. Superrepellency of Underwater Hierarchical Structures on Salvinia Leaf[J]. Proceedings of the National Academy of Sciences, 2020, 117(5): 201900015.
- [14] WANG H, HE M, LIU H, et al. Controllable Water Behaviors on V-Shape Micro-Grooved Titanium Alloy Surfaces Depending on the Depth-to-Width Aspect Ratio [J]. Materials Today Physics, 2021, 20: 100461.
- [15] PENG Q, JIA L, DING Y, et al. Influence of Groove Orientation on Dropwise Condensation on Hydrophobic and Hierarchical Superhydrophobic Surfaces with Microgroove Arrays[J]. International Communications in Heat and Mass Transfer, 2020, 112: 104492.
- [16] FENG L, LI S, LI Y, et al. Super-Hydrophobic Surfaces: from Natural to Artificial[J]. Advanced Materials, 2002, 14(24): 1857-1860.
- [17] ZHENG Y, GAO X, JIANG L. Directional Adhesion of Superhydrophobic Butterfly Wings[J]. Soft Matter, 2007, 3(2): 178-182.
- [18] WENZEL R N. Resistance of Solid Surfaces to Wetting by Water[J]. Industrial & Engineering Chemistry, 1936, 28(8): 988-994.
- [19] CASSIE A B D, BAXTER S. Wettability of Porous Surfaces[J]. Transactions of the Faraday Society, 1944, 40: 546-551.
- [20] ZHENG Q S, YU Y, ZHAO Z H. Effects of Hydraulic Pressure on the Stability and Transition of Wetting Modes of Superhydrophobic Surfaces[J]. Langmuir, 2005, 21(26): 12207-12212.
- [21] MARMUR A. Wetting on Hydrophobic Rough Surfaces: to be Heterogeneous or not to be?[J]. Langmuir, 2003, 19(20): 8343-8348.
- [22] LOU J, SHI S L, MA C, et al. Suspended Penetration Wetting State of Droplets on Microstructured Surfaces[J]. Science China: Physics, Mechanics & Astronomy, 2021, 64(4): 244711.
- [23] BORMASHENKO E, POGREB R, WHYMAN G, et al. Vibration-Induced Cassie-Wenzel Wetting Transition on Rough Surfaces[J]. Applied Physics Letters, 2007, 90(20): 201917.
- [24] SUDEEPTHI A, YEO L, SEN A K. Cassie-Wenzel

- Wetting Transition on Nanostructured Superhydrophobic Surfaces Induced by Surface Acoustic Waves[J]. *Applied Physics Letters*, 2020, 116(9): 093704.
- [25] HE S, MENG Y, TIAN Y. Correlation Between Adsorption/Desorption of Surfactant and Change in Friction of Stainless Steel in Aqueous Solutions Under Different Electrode Potentials[J]. *Tribology Letters*, 2011, 41(3): 485-494.
- [26] CHO H J, MIZERAK J P, WANG E N. Turning Bubbles on and off during Boiling Using Charged Surfactants[J]. *Nature Communications*, 2015, 6: 8599.
- [27] MORTON S A, KEFFER D J, COUNCE R M, et al. Behavior of Oil Droplets on an Electrified Solid Metal Surface Immersed in Ionic Surfactant Solutions[J]. *Langmuir*, 2005, 21(5): 1758-1765.
- [28] KEDZIERSKI J, BERRY S. Engineering the Electrocapillary Behavior of Electrolyte Droplets on Thin Fluoropolymer Films[J]. *Langmuir*, 2006, 22(13): 5690-5696.
- [29] SCHULTZ A, CHEVALLIOT S, KUIPER S, et al. Detailed Analysis of Defect Reduction in Electrowetting Dielectrics through a Two-Layer 'Barrier' Approach[J]. *Thin Solid Films*, 2013, 534: 348-355.
- [30] LOKANATHAN M, SHARMA H, SHABAKA M, et al. Comparing Electrowettability and Surfactants as Tools for Wettability Enhancement on a Hydrophobic Surface[J]. *Colloids and Surfaces: Physicochemical and Engineering Aspects*, 2020, 585: 124155.
- [31] 于力, 邓云, 王丹凤, 等. 表面活性剂对壳聚糖成膜体系物理特性的影响[J]. *包装工程*, 2022, 43(11): 1-7.
- YU Li, DENG Yun, WANG Dan-feng, et al. Effect of Surfactants on Physical Properties of Chitosan Film-forming System[J]. *Packaging Engineering*, 2022, 43(11): 1-7.
- [32] YU Y S, HUANG X, SUN L, et al. Evaporation of Ethanol/Water Mixture Droplets on Micro-Patterned PDMS Surfaces[J]. *International Journal of Heat and Mass Transfer*, 2019, 144: 118708.
- [33] DUTKIEWICZ E, JAKUBOWSKA A. Effect of Electrolytes on the Physicochemical Behaviour of Sodium Dodecyl Sulphate Micelles[J]. *Colloid and Polymer Science*, 2002, 280(11): 1009-1014.
- [34] LIFENG C, MIRIAM G, KELIANG L. A Facile Surfactant Critical Micelle Concentration Determination [J]. *Chemical Commun*, 2011, 47: 5527-5529.
- [35] HUHTAMÄKI T, TIAN X, KORHONEN J T, et al. Surface-Wetting Characterization Using Contact-Angle Measurements[J]. *Nature Protocols*, 2018, 13(7): 1521-1538.
- [36] MUGELE F, HEIKENFELD J. *Electrowetting: Fundamental Principles and Practical Applications*[M]. Weinheim: Wiley-VCH Verlag Gmb H & Co, 2019: 205-206.
- [37] VERHEIJEN H J J, PRINS M W J. Reversible Electrowetting and Trapping of Charge: Model and Experiments[J]. *Langmuir*, 1999, 15 (20): 6616-6620.
- [38] MURAKAMI D, JINNAI H, TAKAHARA A. Wetting Transition from the Cassie-Baxter State to the Wenzel State on Textured Polymer Surfaces[J]. *Langmuir*, 2014, 30(8): 2061-2067.

责任编辑: 彭颀

(上接第 168 页)

- [23] LIU Chao-ran, SUN Jing, ZHUANG Yu, et al. Self-Propelled Droplet-Based Electricity Generation[J]. *Nanoscale*, 2018, 10(48): 23164-23169.
- [24] WANG Shun, LI Hai-long, DUAN Hu, et al. Directed Motion of an Impinging Water Droplet—Seesaw Effect [J]. *Journal of Materials Chemistry A*, 2020, 8(16): 7889-7896.
- [25] LI Juan, QIN Qi hang, SHAH A, et al. Oil Droplet Self-Transportation on Oleophobic Surfaces[J]. *Science Advances*, 2016, 2(6): e1600148.
- [26] 张凯, 陆勇俊, 王峰会. 表面能梯度驱动下纳米水滴在不同微结构表面上的运动[J]. *物理学报*, 2015, 64(6): 272-277.
- ZHANG Kai, LU Yong-jun, WANG Feng-hui. Motion of the Nanodroplets Driven by Energy Gradient on Surfaces with Different Microstructures[J]. *Acta Physica Sinica*, 2015, 64(6): 272-277.
- [27] TUTEJA A, CHOI W, MA Ming-lin, et al. Designing Superoleophobic Surfaces[J]. *Science*, 2007, 318(5856): 1618-1622.
- [28] LIU T “, KIM C J “. Turning a Surface Superrepellent even to Completely Wetting Liquids[J]. *Science*, 2014, 346(6213): 1096-1100.
- [29] HU Song-tao, CAO Xiao-bao, REDDYHOFF T, et al. Liquid Repellency Enhancement through Flexible Microstructures[J]. *Science Advances*, 2020, 6(32): eaba9721.
- [30] XIA Zhen-yan, ZHAO Yang, YANG Zhen, et al. The Simulation of Droplet Impact on the Super-Hydrophobic Surface with Micro-Pillar Arrays Fabricated by Laser Irradiation and Silanization Processes[J]. *Colloids and Surfaces A: Physicochemical and Engineering Aspects*, 2021, 612: 125966.
- [31] LIN Dian-ji, WANG Liang, WANG Xiao-dong, et al. Reduction in the Contact Time of Impacting Droplets by Decorating a Rectangular Ridge on Superhydrophobic Surfaces[J]. *International Journal of Heat and Mass Transfer*, 2019, 132: 1105-1115.
- [32] YANG Cheng-juan, CAO Wei-ran, YANG Zhen. Study on Dynamic Behavior of Water Droplet Impacting on Super-Hydrophobic Surface with Micro-Pillar Structures by VOF Method[J]. *Colloids and Surfaces A: Physicochemical and Engineering Aspects*, 2021, 630: 127634.

责任编辑: 马梦遥